3300 *Chem. Mater.* **2010,** *22,* 3300–3306
DOI:10.1021/cm100702p

CHEMISTRY OF MATERIALS
Article

Direct Observation of Microgel Erosion via in-Liquid Atomic Force Microscopy

Antoinette B. South and L. Andrew Lyon*

School of Chemistry and Biochemistry and Petit Institute for Bioengineering & Bioscience, Georgia Institute of Technology, Atlanta, Georgia 30332-0400

Received March 9, 2010

Degradable hydrogel particles have been integrated into a variety of biomedical applications, but there are no studies to date illustrating the detailed morphological changes that occur in single microgels during erosion in complex media. Herein, we use ambient and in-liquid atomic force microscopy (AFM) to interrogate changes in morphology of substrate-supported microgels synthesized from poly(*N*-isopropylmethacrylamide-*co*-acrylic acid) cross-linked with a hydrolyzable cross-linker (*N*,*O*-dimethacryloyl hydroxylamine). Erosion was monitored under physiological conditions (37 °C in serum-supplemented PBS). At early time points of erosion, the microgel swelling capacity increases due to the hydrolysis of the cross-linker and a concomitant decrease in network connectivity. After longer erosion times and extensive polymer loss, the remnant degraded microgel reveals a high polymer density toward the center of the particle with a low-density corona, which most likely results from internal cross-linking of the polymer. These detailed morphological changes illustrate the complex nature of erodible microgels, which would be difficult to observe using ensemble-averaged analyses.

Introduction

Hydrogels have acquired tremendous interest as components for interfacing with biological environments.[1−3] This is due to their adaptable and dynamic nature, which makes them ideally suited for interacting with a complex and active system. For example, their ability to respond to external stimuli allows their network to dynamically interact with proteins, cells, or tissues for uses such as biosensing or drug delivery.[4−6] Micro- or nanosized hydrogels, which are spherical hydrogel particles that range in size from < 100 nm to a few micrometers in diameter,[7−9] are relevant for biomedical applications where confined environments must be accessed, such as in targeted drug delivery where extended blood circulation and extravasation into tumors is required.[10,11] Microgels also benefit from their utility in the fabrication of complex structures via self-assembly,[12−14] and their high surface-to-volume ratio that maximizes their interaction with the environment. Consequently, microgel-based materials have demonstrated utility in drug delivery,[15] nonfouling films,[16,17] and biosensors.[18]

A large number of the materials used in biomedical applications ultimately need to be cleared from the body after they have provided their specific function, in order to prevent unwanted side effects or chronic accumulation. Thus, biodegradable constructs are of interest where achieving a detailed understanding of the morphological changes that occur during erosion is of particular importance. However, there are no studies that directly monitor degradable hydrogel particles in biologically relevant complex fluids, such as serum, on the single particle scale. In this report, we use atomic force microscopy (AFM) to interrogate the morphological and size changes of degradable poly(*N*-isopropylmethacrylamide-*co*-acrylic acid) (pNIPMAm-AAc) microgels cross-linked with *N*,*O*-dimethacryloyl hydroxylamine (DMHA) when incubated at physiological temperature (37 °C) in serum. The cross-linker DMHA undergoes base-catalyzed hydrolysis and

*Corresponding author. Tel.: (+1) 404-894-4090. Fax: (+1) 404-894-7452. E-mail: lyon@gatech.edu.

(1) Peppas, N. A.; Hilt, J. Z.; Khademhosseini, A.; Langer, R. *Adv. Mater.* **2006**, *18*, 1345.
(2) Ulijn, R. V.; Bibi, N.; Jayawarna, V.; Thornton, P. D.; Todd, S. J.; Mart, R. J.; Smith, A. M.; Gough, J. E. *Mater. Today* **2007**, *10*, 40.
(3) Yoshida, R. *Curr. Org. Chem.* **2005**, *9*, 1617.
(4) Miyata, T.; Uragami, T.; Nakamae, K. *Adv. Drug Delivery. Rev.* **2002**, *54*, 79.
(5) Qiu, Y.; Park, K. *Adv. Drug Delivery. Rev.* **2001**, *53*, 321.
(6) Kuckling, D. *Colloid Polym. Sci.* **2009**, *287*, 881.
(7) Pelton, R. *Adv. Colloid Interface Sci.* **2000**, *85*, 1.
(8) Jones, C. D.; Lyon, L. A. *Macromolecules* **2000**, *33*, 8301.
(9) Gan, D. J.; Lyon, L. A. *J. Am. Chem. Soc.* **2001**, *123*, 7511.
(10) Oh, J. K.; Drumright, R.; Siegwart, D. J.; Matyjaszewski, K. *Prog. Polym. Sci.* **2008**, *33*, 448.
(11) Raemdonck, K.; Demeester, J.; De Smedt, S. *Soft Matter* **2009**, *5*, 707.
(12) Serpe, M. J.; Jones, C. D.; Lyon, L. A. *Langmuir* **2003**, *19*, 8759.
(13) Lynch, I.; Miller, I.; Gallagher, W. M.; Dawson, K. A. *J. Phys. Chem. B* **2006**, *110*, 14581.
(14) Sorrell, C., D.; Lyon, L. A. *Langmuir* **2008**, *24*, 7216.
(15) Blackburn, W. H.; Dickerson, E. B.; Smith, M. H.; McDonald, J. F.; Lyon, L. A. *Bioconj. Chem.* **2009**, *20*, 960−968.
(16) Nolan, C. M.; Reyes, C. D.; Debord, J. D.; Garcia, A. J.; Lyon, L. A. *Biomacromolecules* **2005**, *6*, 2032.
(17) Bridges, A. W.; Singh, N.; Burns, K. L.; Babensee, J. E.; Lyon, L. A.; Garcia, A. J. *Biomaterials* **2008**, *29*, 4605.
(18) Kim, J.; Serpe Michael, J.; Lyon, L. A. *J. Am. Chem. Soc.* **2004**, *126*, 9512.

Published on Web 04/14/2010

has been used as a cross-linker in macrogels and polymeric particles.[19−25] At a pH above 5, hydrolysis of DMHA occurs, and it is therefore a suitable cross-linker for rendering microgels erodible under physiologically relevant conditions.

There are a variety of techniques by which the erosion of degradable particles can be interrogated, such as by monitoring the loss of fluorescent material,[26] drug release,[22,27−29] and molecular weight changes using gel permeation chromatography (GPC).[27,30] Others have also used optical microscopy,[22,27−29,31] interrogated the chemical composition after erosion,[31] or monitored changes in particle light scattering.[31,32] While these methods can provide important information about degradation kinetics, erosion byproducts, and drug release, often it is difficult to monitor degradation in complex media, such as serum, due to interference with the analysis. Furthermore, it is important to understand the detailed morphological changes during erosion, which can only be provided by monitoring those changes at the individual particle level, as opposed to relying on ensemble averaged techniques.

AFM possesses several potential advantages over other techniques for monitoring microgel degradation. One obvious advantage is the possibility for direct observation of how a particle changes at particular time points of erosion and how the changes of a single particle compare to the entire particle population. Furthermore, by using substrate-supported particles, the sample can be incubated in complex media and then be placed in a more controlled environment for subsequent analysis. AFM, in contrast to other common microscopy techniques such as SEM or TEM, can be trivially performed in both dry and liquid environments, which is exceptionally useful in the interrogation of changes in microgel swelling during erosion.

Experimental Section

Materials. All reagents were purchased from Sigma-Aldrich unless otherwise specified. Hydroxylamine hydrochloride, methacryloyl chloride, pyridine (Fischer), chloroform (BDH), and hydrochloric acid (EMD Chemicals Inc.) were all used as received for synthesizing *N*,*O*-dimethacryloyl hydroxylamine (DMHA). The monomer *N*-isopropylmethacrylamide (NIPMAm) was recrystallized from hexanes (J.T. Baker) and dried under vacuum prior to use. The comonomer acrylic acid (AAc), surfactant sodium dodecyl sulfate (SDS), initiator ammonium persulfate (APS), buffer chemicals sodium dihydrogen phosphate monohydrate (Fisher Scientific), glacial acetic acid (Fischer Scientific), formic acid (EMD Chemicals Inc.), sodium chloride (Mallinckrodt), potassium chloride (J.T. Baker), sodium hydroxide, sodium azide, and the surface modification reagent 3-aminopropyl trimethoxysilane (APTMS, TCI America) were used as received. Fetal bovine serum was purchased from Atlanta Biologicals, kept frozen until ready for use, and then aliquots were thawed at room temperature before use. Glass disks of 12-mm diameter were purchased from Bellco Glass. Acetone, isopropyl alcohol, and Absolute 200 proof ethanol (EMD Chemicals Inc.) were used as received. All water used throughout this investigation was house distilled and then deionized to a resistance of at least 18 MΩ (Barnstead Thermolyne E-Pure system).

DMHA Synthesis. *N*,*O*-Dimethacryloyl hydroxylamine (DMHA) was synthesized as described previously.[19] Briefly, 10.1019 g of hydroxylamine hydrochloride (0.145 mol) was placed in a 500 mL round-bottom flask and purged with N_2 gas for approximately 20 min to remove moisture. Pyridine, 50 mL, was added by syringe and stirred with the hydroxylamine hydrochloride salt until completely dissolved. Methacryloyl chloride, 23.52 mL (0.243 mol), was slowly added dropwise while maintaining the solution under nitrogen and in an ice bath. The temperature of the reaction mixture was kept below 30 °C, and 10 mL more pyridine was added to the solution after all the methacryloyl chloride was added. The reaction was then stirred for an additional 4.5 h. Conversion of methacryloyl chloride to product was monitored by thin layer chromatography using a chloroform mobile phase and iodine stain. After complete conversion, 100 mL of chloroform was added, and the solution turned a transparent yellow-brown color. Afterward, 21 mL of hydrochloric acid (15 M) was slowly added dropwise while the solution was maintained in an ice bath. Vapor formed, and the mixture turned turbid. The solution was then poured into a separatory funnel, and 100 mL of deionized water was added. The solution was washed with 100 mL portions of deionized water until the aqueous layer became clear (four washes). The organic layer was then dried over magnesium sulfate and filtered. Chloroform was removed by rotary evaporation, and then, the yellow/brown translucent oil product was dried overnight on a Schlenk line. The product was an off-white solid after drying (7 g isolated). Experimental yield was approximately 34%. The chemical composition of DMHA was determined using a Varian Unity 300 MHz NMR spectrometer and a Perkin-Elmer Series II 2400 CHNS/O Analyzer (see the Supporting Information).

Microgel Synthesis. Microgels were synthesized by free radical precipitation polymerization using a total monomer concentration of 140 mM, in a molar ratio of 96% NIPMAm, 2% DMHA, and 2% AAc. The initiator ammonium persulfate (APS) and surfactant sodium dodecyl sulfate (SDS) were both used at an 8 mM concentration. The cross-linker DMHA was first dissolved in 5 mL of DMSO, while the rest of the reagents were dissolved in 45 mL of deionized water. The water and DMSO solutions were mixed and filtered through Whatman #2 filter paper via a vacuum filtration system. The polymerization was allowed to proceed for approximately 4 h at 70 °C under a N_2 blanket.

(19) Ulbrich, K.; Subr, V.; Seymour, L. W.; Duncan, R. *J. Controlled Release* **1993**, *24*, 181.
(20) Ulbrich, K.; Subr, V.; Podperova, P.; Buresova, M. *J. Controlled Release* **1995**, *34*, 155.
(21) Akala, E. O.; Kopeckova, P.; Kopecek, J. *Biomaterials* **1998**, *19*, 1037.
(22) Yin, W. S.; Akala, E. O.; Taylor, R. E. *Int. J. Pharm.* **2002**, *244*, 9.
(23) Horak, D.; Kroupava, J.; Slouf, M.; Dvorak, P. *Biomaterials* **2004**, *25*, 5249.
(24) Chivukula, P.; Dusek, K.; Wang, D.; Duskova-Smrckova, M.; Kopeckova, P.; Kopecek, J. *Biomaterials* **2006**, *27*, 1140.
(25) Pradny, M.; Michalek, J.; Lesny, P.; Hejcl, A.; Vacik, J.; Slouf, M.; Sykova, E. *J. Mater. Sci.: Mater. Med.* **2006**, *17*, 1357.
(26) Nayak, S.; Gan, D. J.; Serpe, M. J.; Lyon, L. A. *Small* **2005**, *1*, 416.
(27) Zolnik, B. S.; Leary, P. E.; Burgess, D. J. *J. Controlled Release* **2006**, *112*, 293.
(28) Bulmus, V.; Chan, Y.; Nguyen, Q.; Tran, H. L. *Macromol. Biosci.* **2007**, *7*, 446.
(29) Goh, S. L.; Murthy, N.; Xu, M. C.; Frechet, J. M. J. *Bioconj. Chem.* **2004**, *15*, 467.
(30) Gao, D.; Xu, H.; Philbert, M. A.; Kopelman, R. *Nano Lett.* **2008**, *8*, 3320.
(31) Huang, X.; Misra, G. P.; Vaish, A.; Flanagan, J. M.; Sutermaster, B.; Lowe, T. L. *Macromolecules* **2008**, *41*, 8339.
(32) Smith, M. H.; South, A. B.; Gaulding, J. C.; Lyon, L. A. *Anal. Chem.* **2009**, *82*, 523.

Particle Characterization. Dynamic light scattering (DLS) was used as previously described,[33,34] to measure the hydrodynamic radius and diffusion coefficient of synthesized particles. Microgel dispersions were prepared in cold (3 °C) 1X PBS and pH 3 formate buffer of the same ionic strength. A Protein Solutions DynaPro equipped with a temperature-controlled microsampler was used. Light scattering data was collected at 3 °C at an interval of 10 s per reading with a photodiode detector fixed at 90° relative to the incident the laser light (783.9 nm). Dynamics Software was used to calculate the autocorrelation decay from the random fluctuations in scattered light intensity. This information was then used to determine the diffusion coefficient of the sample in solution, which correlates with the hydrodynamic radius of the particles using the Stokes−Einstein equation. Scattering intensity measurements were performed on a steady-state fluorescence spectrophotometer (Photon Technology International), equipped with a Model 814 PMT photon-counting detector. Scattering was monitored at an excitation and emission wavelength of 600 nm and the temperature was increased from 25 to 50 °C at a ramp rate of 0.5 °C/min.

Sample Preparation. Glass coverslip disks, 12-mm diameter, were placed in a ceramic glass slide holder and cleaned using a sequential solvent sonication method. A sequential solvent sonication method proceeded with the following solvent sequence using a Bransonic 2510 Ultrasonicator (42 kHz ± 6% output): 30 min in dilute soapy (Alconox) water, 15 min in deionized water, 15 min in acetone, 15 min in absolute ethanol, and 15 min in isopropyl alcohol. Afterward, the glass was immediately equilibrated for 30 min in absolute ethanol and 1% by volume APTMS was added. The glass was incubated with the APTMS−ethanol solution for 2 h under gentle agitation. The glass was then rinsed with a 70% aqueous ethanol solution and deionized water, and then dried under a gentle stream of N_2.

Microgels were dispersed at a concentration of 0.1 mg/mL in high ionic strength (100 mM) pH 5 acetic acid buffer containing 1 ppm sodium azide. While microgels were dispersing prior to film deposition, they were kept on a shaker table under refrigeration to ensure that no premature degradation was occurring. Cleaned and dried glass disks were individually placed at the bottom of 24-well plates and 500 μL of pH 5 high ionic strength acetic acid buffer was immediately added. The glass was allowed to equilibrate for 30 min, and the buffer was then replaced with 500 μL of the microgel solution. Films were generated by centrifugation deposition[35] at 2250*g* for 5 min. Afterward, the films were briefly rinsed with DI water and dried under a gentle N_2 stream.

Degradation Studies. Degradable microgel films were incubated in one of four different aqueous environments: (1) 1X PBS-supplemented serum at 37 °C, (2) pH 3 buffer at 37 °C, (3) 1X PBS-supplemented serum at room temperature, and (4) pH 3 buffer at room temperature. To make the PBS-supplemented serum, 1X PBS was first prepared by preparing a solution that contained 10 mM dihydrogen phosphate (24 mM ionic strength), 137 mM NaCl, and 2.7 mM KCl in deionized water, followed by titration to a pH of 7.4. Fetal bovine serum was then diluted to a 10% by volume solution with 1X PBS; this solution was used directly for degradation studies. To make the pH 3 buffer, a solution of 10 mM formic acid was prepared, to which NaCl was added to make the ionic strength 24 mM. Then 137 mM NaCl and 2.7 mM KCl were dissolved in the formic acid−NaCl solution and titrated to a pH of 3. Prior to incubation with microgel films, the buffer was diluted to a 10% by volume solution with deionized water to yield a similar salt content to that of the PBS-supplemented serum.

Scheme 1. Erosion of DMHA Cross-Linked Microgels

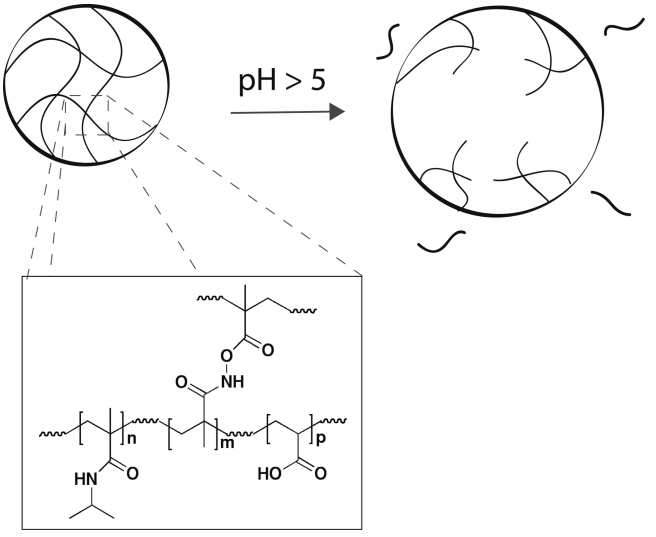

Atomic Force Microscopy and Image Analysis. At a specified time, the film was removed from the incubation solution, rinsed with DI water, and dried with a gentle stream of N_2 prior to analysis. Each sample was characterized using an Asylum Research MFP-3D atomic force microscope. Imaging was performed and processed using the MFP-3D software written in the IgorPro (WaveMetrics Inc., Lake Oswego, OR) environment. For imaging under dry conditions, noncontact mode aluminum-coated silicon nitride cantilevers (force constant = 42 N/m, resonance frequency = 320 kHz), purchased from NanoWorld, were used. Three separate images were taken for each sample, and the average particle height was calculated from 10 particles in each image. Particle heights were determined by drawn line profiles using the analysis panel in the MFP3D software. Lines were drawn across the center of the particle, and the height was measured from the center of the particle to the lowest point on the surface background. In-liquid imaging was performed using an Asylum Research iDrive cantilever with an integrated circuit loop (force constant = 0.09 N/m, resonance frequency = 32 kHz in air) positioned on a specially designed holder (purchased from Asylum Research). This holder is equipped with two electrically isolated and conductive spring clips that supply a voltage to actuate the cantilever. Actuation of the cantilever occurs via a magnetic field coupled to an applied oscillating current, through the cantilever, that produces an orthogonal Lorentzian force. A drop of 10 mM pH 5 low ionic strength (24 mM) acetic acid buffer was placed on the microgel film, with the iDrive cantilever lowered into the drop, for 30 min to equilibrate before proceeding to take the image in liquid.

Results and Discussion

Microgels composed of pNIPMAm-AAc cross-linked with DMHA are illustrated in Scheme 1. This particular chemical composition was chosen to ensure microgel erosion under physiological conditions (37 °C, pH 7.4, in serum), as opposed to other degradable constructs that

(33) Yi, Y. D.; Bae, Y. C. *J. Appl. Polym. Sci.* **1998**, *67*, 2087−2092.
(34) Debord, J. D.; Lyon, L. A. *J. Phys. Chem. B* **2000**, *104*, 6327.
(35) South, A. B.; Whitmire, R. E.; García, A. J.; Lyon, L. A. *ACS Appl. Mater. Interfaces* **2009**, *1*, 2747.

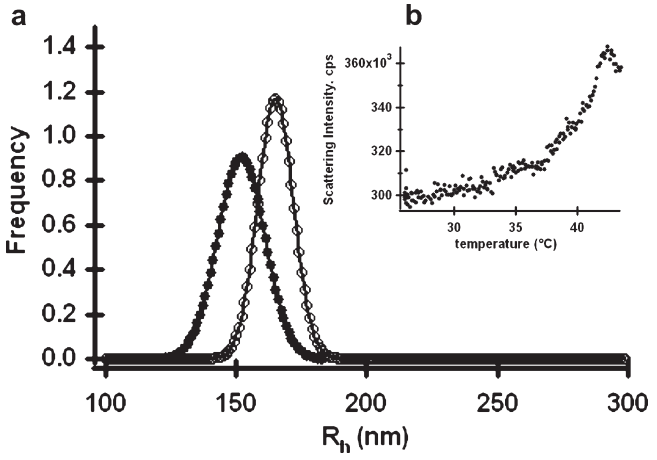

Figure 1. (a) Size distribution of degradable microgel hydrodynamic radii (R_h) determined by DLS (cumulants fit) at pH 3 (filled circles) and pH 7.4 (open circles) and (b) temperature-dependent microgel scattering intensity in pH 3 buffer.

require acidic excursions from physiologic pH to induce rapid erosion.[36,37] The cross-linker DMHA is known to undergo base catalyzed hydrolysis at pH values above 5, thus making it a useful cleavable cross-linker at a physiological pH of 7.4. The copolymerization of AAc into the network enabled the microgels to be Coulombically attached to an amine-functionalized surface in order to monitor erosion of particles affixed to a substrate. The small amount of incorporated AAc (2 mol %) contributes only slightly to a pH-dependent swelling (Figure 1a). Lastly, the polymer pNIPMAm undergoes a transition from a water-swollen to a deswollen state upon an increase in temperature above ~41 °C. Thus, these particles are solvent swollen at 37 °C. The thermoresponsive behavior of these microgels can be seen from the temperature dependent turbidity curve in Figure 1b.

After deposition, the degradable microgels were incubated either in the PBS-supplemented serum (pH 7.4) or in the control pH 3 buffer solution. Erosion was monitored over time either at 37 °C or room temperature. AFM scans were taken in both dry and in liquid (pH 5 buffer) environments at specific time points to evaluate the erosion and change in particle swelling with time. Typical particle erosion over time at 37 °C under dehydrated and hydrated conditions is shown in Figure 2. When imaged dry before commencing erosion (Figure 2a), the substrate-attached microgels appear hemispherical in shape. After 24 h of exposure to serum, the microgels decrease in height due to the loss of polymer (Figure 2b), and after 434 h of exposure, the microgel appears to have largely dissolved away, with the exception of a region of high polymer density concentrated in the center of the particle (Figure 2c). These particles also appear to exhibit a low-density polymer "ghost" radiating from the dense polymer center. This halo of low polymer density is observed surrounding all microgels after extensive erosion (see the Supporting Information) and is approximately the size of the particle's original footprint area. We tentatively attribute the presence of a dense, nondegradable core to the presence of pNIPMAm self-cross-linking. Gao and Frisken have observed similar internal cross-linking in poly(*N*-isopropylacrylamide) gel nanospheres, which they attributed to a chain transfer mechanism.[38] These authors observed nanospheres of pNIPAm, rather than just linear polymer, when NIPAm was polymerized with a free radical initiator above the phase transition temperature in the absence of cross-linking monomers. Therefore, self-cross-linking most likely occurred and is explained by chain transfer of two active hydrogen atoms that could be attacked by free radicals: the hydrogen on the tertiary carbon of the isopropyl group and the hydrogen on the tertiary carbon on the main chain backbone. This same self-cross-linking could also have occurred for the pNIPMAm microgels discussed here, thus explaining the presence of a dense nonerodible polymer core after extensive erosion.

When hydrated, microgels swell to more than twice their height compared to their dehydrated height at all time points during erosion (Figure 2d−f). The microgel diameter in Figure 2d, before erosion has commenced, is consistent with the microgel size when suspended in solution; the hydrodynamic radius (R_h) is approximately 133 ± 6 nm (21 ± 3% PD) in pH 5 buffer. Furthermore, as was observed for microgel erosion under dehydrated conditions, an overall decrease in particle height during erosion is also observed for the microgels when imaged in liquid. The aforementioned low polymer density corona around the dense microgel center observed after 434 h of erosion is also more clearly visible when hydrated (Figure 2f). In addition to the observed changes in particle structure, the background glass substrate becomes noticeably covered with material, which is likely polymer that has detached from the microgels during erosion or protein components from the serum. Due to the slight negative charge of the polymer from acrylic acid, the dissociated polymer chains likely do not readsorb onto the microgels, but instead adsorb onto the cationic glass background after release from the microgel.

In addition to the inspection of individual particles, the imaging of multiple microgels allows for observations of the heterogeneity of the entire sample. Larger area scans of the microgel monolayers illustrate that the microgels present within a particular film erode at a uniform rate with uniform changes in particle morphology and swelling. Images illustrating the uniformity of the microgel samples can be found in the Supporting Information.

The average dehydrated particle heights as a function of time are shown in Figure 3. Erosion at room temperature and 37 °C under both eroding (pH 7.4) and noneroding (pH 3) conditions are compared here. First, these data clearly display a temperature dependence to the erosion, with the rate being accelerated at higher temperatures, which has been observed previously by our

(36) Murthy, N.; Thng, Y. X.; Schuck, S.; Xu, M. C.; Frechet, J. M. J. *J. Am. Chem. Soc.* **2002**, *124*, 12398.
(37) Lee, E. S.; Gao, Z. G.; Bae, Y. H. *J. Controlled Release* **2008**, *132*, 164.
(38) Gao, J.; Frisken, B. J. *Langmuir* **2003**, *19*, 5212.

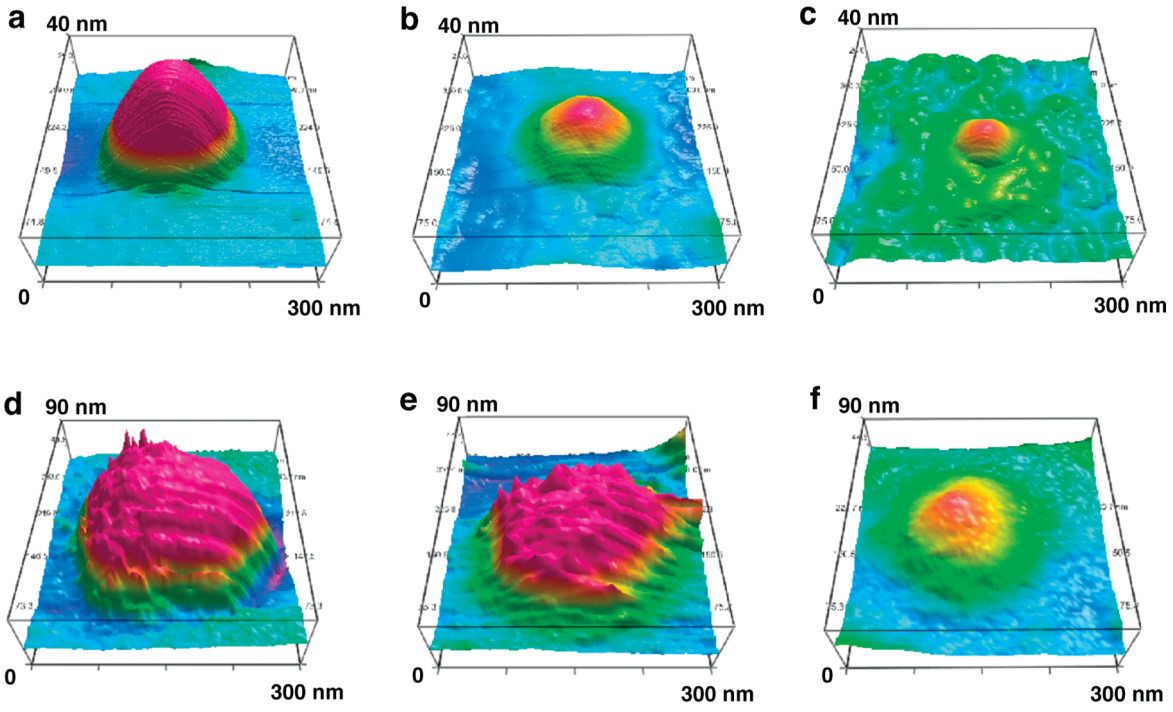

Figure 2. Three-dimensional renderings of AFM images obtained from a single microgel during erosion at 0 (a, d), 24 (b, e), and 434 h (c, f). Images were taken under dehydrated (a−c) or hydrated (d−f) conditions.

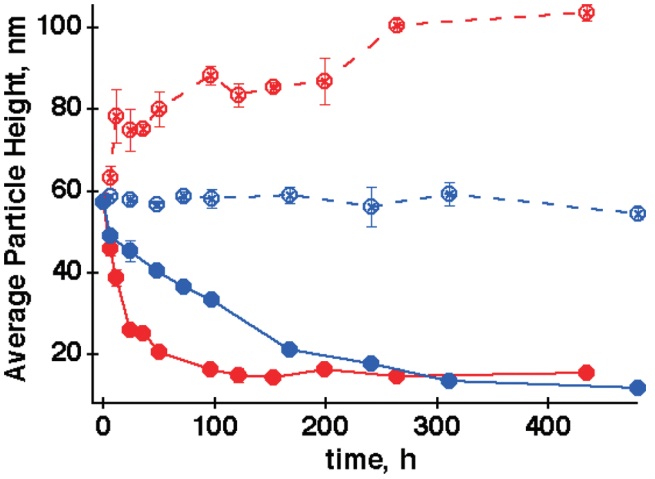

Figure 3. Average microgel height over time under dry imaging conditions. Data represents microgel erosion in serum at 37 °C (filled red circles) and room temperature (filled blue circles), and in pH 3 control buffer at 37 °C (open red circles) and room temperature (open blue circles). Error bars represent the standard deviation of the average particle height measured over three separately scanned images.

group and others.[27,32] Degradation appears to level off at ~100 and 300 h at 37 °C and room temperature, respectively. In pH 3 buffer at room temperature, the microgel height remains constant over time, but at 37 °C, there is a marked increase in particle height at early time points (after 6 h), which continues to a slow and steady increase over time. We hypothesize that upon incubation at a higher temperature (37 °C) at pH values where the AAc moieties are protonated, there may be some partial desorption of the microgels from the substrate over time. Indeed, microgels incubated under these conditions appear to have a smaller footprint area, which is perhaps indicative of weaker substrate−particle interactions and therefore less substrate-induced deformation (see Supporting Information). Note that it is unlikely that the pH-dependent erosion exhibited here is affected by the small amount of acrylic acid comonomer. We have shown previously that microgels not containing AAc also erode at pH values above 5 and do not erode when dispersed in a low pH environment (pH 3).[32] Furthermore, lack of erosion observed for these microgels in pH 3 buffer cannot be attributed to protonated side chains because the decreased microgel hydrodynamic radius, compared to pH 7.4 buffer (Figure 1), is not sufficient to prevent erosion completely. The pH-dependent erosion is largely attributed to the pH-dependent hydrolysis of the DMHA cross-linker.[19,20]

To observe microgel swelling at different time points during erosion, AFM was performed in liquid using a selection of the same microgel films used for dry measurements (Figure 4). In general, there is once again a decrease in the average particle height over time at pH 7.4, and again, degradation is accelerated by an increase in temperature. Control samples (pH 3) do not show significant loss of swollen microgel height over time (see Supporting Information). It is also clear from these data that the microgel ensemble exhibits swelling behavior in a uniform fashion. Because swelling behavior in hydrogel materials is dictated by the connectivity and composition of the polymeric network, it is expected that during chain scission of the DMHA cross-linker these microgels will display increased swelling behavior over time. Though this phenomenon is often difficult to observe when polymer mass loss is occurring simultaneously, at early time points during erosion excess swelling can be observed. For example, after 6 h of erosion at room temperature, there is an approximately 14% height decrease when imaging is

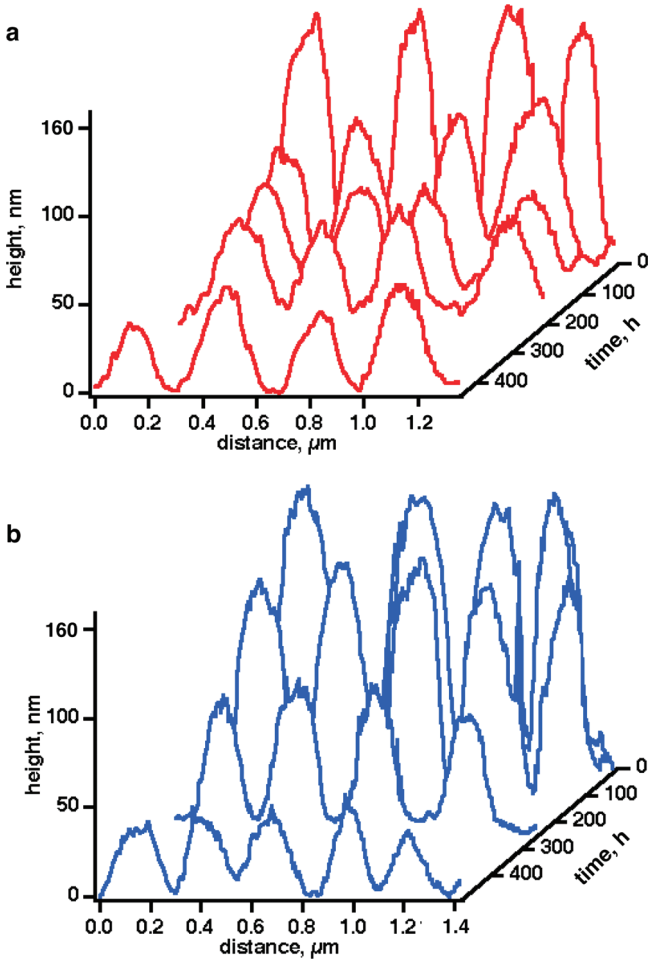

Figure 4. AFM height line profiles taken from an ensemble of hydrated microgels at different time points in serum at (a) 37 °C and (b) room temperature.

performed under dehydrated conditions. However, when the microgels are interrogated following swelling, the height of the partially eroded microgels actually increases slightly relative to the nondegraded particles. This is clearly illustrated by the data shown in Figure 5 where mass loss from the microgels is clearly observable in the dry images, but upon swelling the particles appear taller. These data highlight a critical issue in the measurement of erosion via ensemble-averaged techniques. For example, if particle size in the swollen state were used as the main indicator of particle erosion (e.g., by dynamic light scattering measurements), the loss of particle mass would appear to be balanced by cross-link scission and concomitant particle swelling at early erosion time points. In other words, the microgel size would appear to stay constant or possibly even increase as erosion proceeded, with large decreases in size only being observable late in the erosion process. Obviously, size alone is a poor metric by which to judge the rate of microgel erosion. Additional difficulties would also arise in the data interpretation when one considers the decrease in scattering intensity that would accompany particle erosion, making the determination of particle size significantly less reliable as the erosion proceeds. Furthermore, the study of microgel erosion by dynamic light scattering, turbidity, multiangle static light scattering, or fluorescence would certainly be difficult to perform in the presence of solvated linear polymer that had sloughed off the remaining microgels, as it would present a significant background signal against which the intact microgel signal would be difficult to measure. Such background issues are even more problematic in complex media such as serum. Finally, serum components might even cause aggregation of the erosion

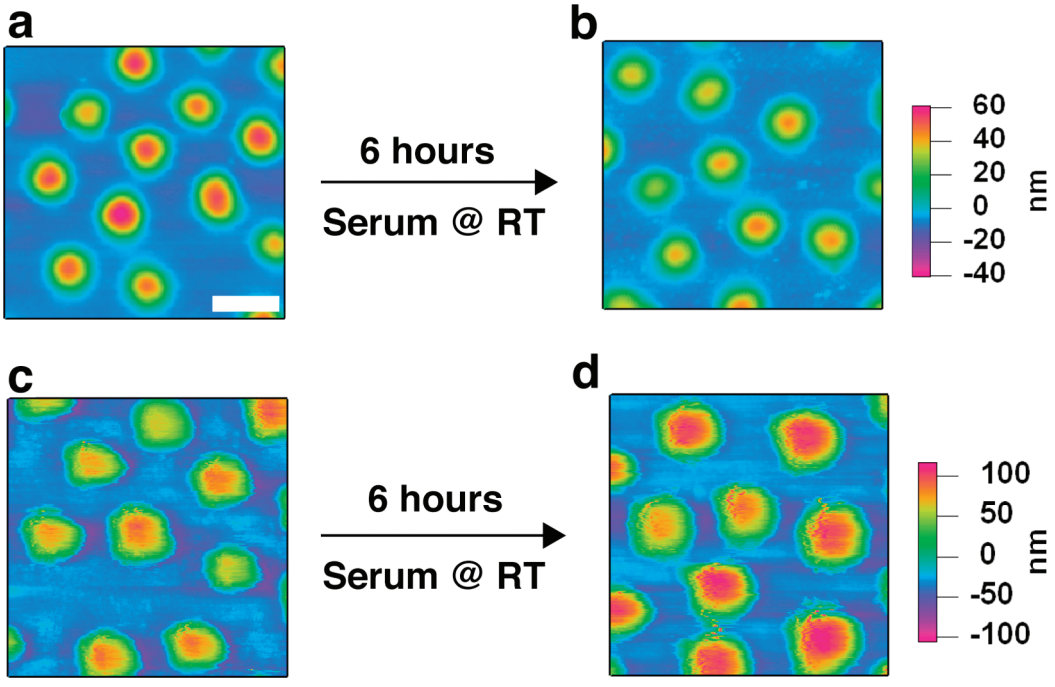

Figure 5. Two-dimensional height images of microgel erosion at room temperature imaged under dry conditions (a, b) and in liquid (c, d). Time points of time 0 (a, c) and 6 h in serum (b, d) are shown. The scale bar represents 250 nm.

products or remnant microgels, making analysis even more difficult. Together, these issues illustrate the numerous problems associated with microgel erosion analysis via ensemble-averaged techniques performed on microgel dispersions, and highlight the utility of probe microscopy as an alternative characterization tool.

Conclusion

Understanding the fate of degradable microgels under physiological conditions is potentially important for their application to various biomedical problems. The erosion process involves loss of polymer, changes in particle swelling, and decreased colloidal stability, with complex environments such as serum adding to these complications. Current techniques used to monitor microgel erosion suffer from these complications and, in addition, only reveal ensemble-averaged information about the sample. In this work, atomic force microscopy was used to interrogate microgels during erosion in physiologically relevant complex media (serum) on a single particle scale, while simultaneously showing that single-particle changes are indicative of the sample as a whole. Additionally, the ability to interrogate microgel erosion over time under both dehydrated and hydrated conditions allowed for direct and coexistent observations of microgel polymer loss and network swelling associated with cross-linker scission. Importantly, the morphological changes of erodible microgels shown here could only be effectively observed using single particle analysis.

Acknowledgment. We acknowledge financial support via Georgia Institute of Technology GTEC II funds. A.B.S is supported in part by the TI:GER (Technological Innovation: Generating Economic Results) program at Georgia Tech. We also thank Ms. Danya Tai for contributing to the synthesis of degradable microgels.

Supporting Information Available: Additional AFM images and analyses and chemical composition analysis (^{1}H NMR and elemental analysis) of the DMHA cross-linker. This material is available free of charge via the Internet at http://pubs.acs.org.